Cysteine radical cation: A distonic structure probed by gas phase IR spectroscopy

Rajeev K. Sinha,[a] Philippe Maître,[a] Susanna Piccirillo,[b] Barbara Chiavarino,[c] Maria Elisa Crestoni[c] and Simonetta Fornarini*[c]

Received 24th February 2010, Accepted 26th April 2010
DOI: 10.1039/c003576a

The interest in the radical cations of amino acids is twofold. On the one hand, these species are relevant in enzymatic catalysis and in oxidative damage of proteins. On the other hand, as constituents of peptides and proteins, they aid the mass spectrometric characterization of these biomolecules, yielding diagnostic fragmentation patterns and providing complementary information with respect to the one obtained from even electron ions. The cysteine radical cation has been obtained by S–NO bond cleavage of protonated S-nitrosocysteine and thoroughly characterized by IRMPD spectroscopy, both in the 1000–2000 cm^{-1} range (the highly structurally diagnostic, so-called 'fingerprint' range) and in the 2900–3700 cm^{-1} spectral range, encompassing O–H and N–H stretching vibrations. In this way the distonic structure in which the charge is on the NH_3 group and the spin is on the sulfur atom is unambiguously demonstrated. This tautomer is a local minimum on the potential energy surface, at 29.7 kJ mol^{-1} with respect to the most stable tautomer, a captodative structure allowing extensive delocalization of charge and spin.

Introduction

Many important processes in protein chemistry comprise oxidation–reduction reactions in which electron (and proton) transfer processes lead to amino acid radical and radical cation intermediates. Consequently, extensive efforts have been devoted to characterizing amino acid redox cofactors by both experimental and theoretical approaches.[1] However, operating with natural proteins may present serious difficulties due to the size and complexity of amino acid radical enzymes, hampering for example electrochemical and spectroscopic measurements. Operating in a quite different, highly essential environment, namely the gas phase, presents interesting advantages due to the absence of any complicating effects that will affect and determine to a large extent the structural and reactivity features in biological media. In mass spectrometry the radical cations of amino acids can be exploited for characterizing peptides and proteins by means of diagnostic fragmentation patterns.[2] The radical cations of amino acids were typically obtained by thermal desorption of the neutral and electron ionization[3] or by laser ablation followed by UV photoionization.[2,4] Odd-electron ions from multiprotonated peptides are obtained by electron capture which leads to subsequent fragmentation.[5] An important route to amino acid radical cations has been reported to ensue by the reaction of hydroxylamine radical cation with carboxylic acids, suggesting a possible pathway to forming these species in interstellar environment.[6]

The current methods used to form radical cations of various biomolecules including amino acids and peptides rely on the collision induced dissociation (CID) of ternary metal complexes (typically copper(II), $[Cu^{II}(L)(M)]^{\bullet 2+}$, where L is an auxiliary ligand and M an amino acid or peptide).[7] The CID process involves an electron transfer event leading to $M^{\bullet +}$. Alternatively, even electron ions may undergo CID by activating the homolytic cleavage of a weak bond. In particular, the cleavage of the S–NO bond in the protonated species of S-nitrosopeptides is found to be a facile process leading to radical ions with characteristic fragmentation patterns, potentially useful for the analysis of NO-modified proteins.[8] The cysteine radical cation plays an important role in these processes and the NO-cleavage route has been exploited to provide access to this rather elusive species.[9] Indeed, attempts to form the cysteine radical cation by oxidative dissociation of Cu(II) ternary complexes are reported (and also verified by us) to be unsuccessful, in contrast with the closely related methionine, α-methylmethionine and S-methylcysteine radical cations that are generated by oxidative dissociation of $[Cu^{II}(CH_3CN)_2(M)]^{\bullet 2+}$ complexes.[10] The radical cation of cysteine, one of the most easily oxidized amino acids, is rather obtained by Ryzhov *et al.*[9] from protonated S-nitrosocysteine. This species may be formed in solution by a transnitrosylation reaction of cysteine by a nitric oxide donor and then transferrence to the gas phase by electrospray ionization (ESI) or in the gas phase reaction of protonated cysteine with *t*-butylnitrite. Formed in either way, the protonated nitrosocysteine ion is prone to undergoing homolytic NO cleavage yielding a radical cation $Cys^{\bullet +}$ that has been studied by CID mass spectrometry, deuterium labelling experiments and DFT calculations.[9] The potential energy

[a] *Laboratoire de Chimie Physique, UMR8000 Université Paris-Sud 11, Faculté des Sciences d' Orsay, Batiment 350, 91405 Orsay Cedex, France*
[b] *Dipartimento di Scienze e Tecnologie Chimiche, Università di Roma "Tor Vergata", via della Ricerca Scientifica, 00133, Roma, Italy*
[c] *Dipartimento di Chimica e Tecnologie del Farmaco, Università di Roma "La Sapienza", P.le A. Moro 5, 00185, Roma, Italy. E-mail: Simonetta.fornarini@uniroma1.it; Fax: (+39) 06-4991-3602*

profile suggests that the loss of NO from protonated S-nitrosocysteine (the proton placed on the amino group) to form a distonic radical cation is kinetically favoured (eqn (1)).[9]

$$H_3N^+CH(CH_2SNO)CO_2H \rightarrow H_3N^+CH(CH_2S^\bullet)CO_2H + NO^\bullet \quad (1)$$

The so-formed cysteine radical cation ($Cys^{\bullet +}$) has been characterized by studying the dissociation pathways under activation by low energy collisions. The major competing fragmentation paths involve losses of CH_2S and $^\bullet COOH$ and the potential energy profiles have been obtained by DFT calculations. An overall consistent view with regard to the $H_3N^+CH(CH_2S^\bullet)CO_2H$ structure that is assumed for $Cys^{\bullet +}$ has been obtained. However, a more conclusive structural assay such as the one that may be provided by IR spectroscopy is lacking. This is the purpose of the present study aimed at obtaining direct information on the structure of $Cys^{\bullet +}$ ions formed by cleavage of NO from protonated S-nitrosocysteine. To this end the IR spectral features of the gaseous $Cys^{\bullet +}$ ion have been recorded using infrared multiple photon dissociation (IRMPD) spectroscopy. The use of IRMPD spectroscopy for obtaining structural information on gaseous ions is gaining widespread recognition and is increasingly exploited, aided by the availability of widely tunable and powerful sources of IR radiation such as free electron lasers (FEL) and OPO/OPA laser sources. Recent reviews describe the methodology and a number of applications directed to gaining structural information on a variety of species including small organic ions, metal–small organic complexes, biomolecular ions (aminoacids, peptides, proteins, oligosaccharides), and finally bare and solvated ionic complexes, proton or metal cationized.[11] To cite few examples from our work, we have reported the first FEL-FT-ICR study of protonated benzene, obtaining conclusive evidence on the σ-complex structure,[12] while subsequent studies were focussed on positively and negatively charged complexes of aromatic compounds and on biologically relevant ions such as the nitrosyl complex of the heme prosthetic group.[13] Not only has IRMPD spectroscopy proven valuable in characterizing the even electron ions obtained from deprotonation of or proton/metal ion attachment to various amino acids[14] but it has recently allowed to establish a captodative α-radical ion structure for histidine radical cation in the gas phase.[15] In the present contribution the IR spectral features of $Cys^{\bullet +}$ have been ascertained in the gas phase inspecting both the 1000–2000 cm^{-1} range ("fingerprint" region) and the 2900–3700 cm^{-1} spectral range (O–H/N–H stretching region).

Experimental

1. Chemicals

(L)-Cysteine hydrochloride ($CysH^+Cl^-$) was purchased from Sigma-Aldrich whereas other products, such as $NaNO_2$ (97%) and methanol (HPLC grade), were obtained from other commercial sources and used as received. The reaction of cysteine with sodium nitrate in solution has been the subject of several studies.[16] Solutions were prepared by mixing equimolar quantities of $CysH^+Cl^-$ (2 mM) and $NaNO_2$ (2 mM) in 50 : 50 : 1 (v/v/v) water–methanol : sulfuric acid and allowing the development of a red coloured solution, then stored at −20 °C. The mixture was further diluted up to approximately 5 μM concentration by using equal proportions of methanol and water. This diluted solution was injected into the electrospray ionization (ESI) source at 3 μL min^{-1} flow rate. The mass analysis showed cysteine radical cation (*m*/*z* 121), protonated S-nitrosocysteine (*m*/*z* 151), and protonated cystine, the dimeric amino acid formed by the oxidation of two cysteine residues, (*m*/*z* 241) as the prominent components in the solution.

In the present spectroscopic study, cysteine radical cation ($Cys^{\bullet +}$) was formed by two different methods. In the first method, it was formed directly in the ESI process from the reaction mixture described above, whereas in the second method, $Cys^{\bullet +}$ was obtained in the gas phase *via* the loss of NO from mass-selected protonated S-nitrosocysteine upon CID. As illustrated in a following section, the IRMPD spectra obtained for $Cys^{\bullet +}$ formed either directly from the solution or from the CID of protonated S-nitrosocysteine did not show any difference in terms of IR bands. This finding suggests the formation of same ionic species irrespective of the method of formation.

2. IRMPD experiments

IRMPD experiments on cysteine radical cation were performed using the FEL beamline at the Centre Laser Infrarouge Orsay (CLIO) and an OPO/OPA laser system. The FEL system is based on a 16–48 MeV linear electron accelerator which injects bunches of electrons in the alternating magnetic field placed in the optical cavity. Wavelength tunability of this laser system is achieved at fixed electron energy by changing the gap between magnets. For the experiments in the 1000–2000 cm^{-1} spectral region, the electron energy was fixed at 45 MeV and a stable average power of 800–900 mW was observed. The laser-wavelength profile was monitored while recording the spectra with a monochromator associated to a liquid nitrogen cooled HgCdTe detector. The band width of IR-FEL is 0.4–0.5% of the central wavelength. A modified quadupole Paul ion trap (Bruker, Esquire 3000+) is used for the FEL based experiments. The IR-FEL beam was mildly focused in the trap through a ZnSe Brewster window and a conical hole (1 mm diameter) in the ring electrode. Multistage mass spectrometry is performed using the standard Bruker Esquire Control (v 5.2) software. Cysteine radical cations were mass-selected and accumulated for 20 ms prior to IR irradiation. IRMPD on mass selected and accumulated ions was performed using the MS2 step, keeping the excitation amplitude zero to avoid any collision-induced fragmentation. Post-irradiation mass spectra were recorded after four accumulations and this sequence was repeated four times at each photon energy.

In another experimental apparatus, assembled at the Università di Roma "La Sapienza", an Optical Parametric Oscillator/Amplifier (OPO/OPA, LaserVision) is now coupled to a Paul ion trap mass spectrometer (Esquire 6000+, Bruker). This arrangement was inspired by a quite similar system constructed at the Laboratoire de Chimie Physique, Université Paris-Sud 11,[17] and is presently employed to explore the 2900–3700 cm^{-1} spectral region of cysteine radical cation.

The parametric converter is pumped by a non seeded Nd:YAG laser (Continuum Surlite II) operating at 10 Hz repetition rate. The typical pulse width of this pump laser is 4–6 ns with output pulse energy of 600 mJ at 1064 nm. The OPO/OPA laser is tunable from 2000 to 4000 cm^{-1} and tunability is achieved by angle tuning of OPO and OPA crystals simultaneously. The angle tuning is controlled precisely, using software controlled stepping motors. The typical output energy from OPO/OPA was 27–28 mJ $pulse^{-1}$ in the spectral range of investigation with 3–4 cm^{-1} bandwidth. The mid IR output from OPO/OPA is steered in the ion trap using a gold coated plane mirror and is focussed loosely using an MgF_2 lens of focal length 37 cm. IR beam focussing is performed to achieve better overlap with the trapped ion cloud. In the trap, ions were accumulated for 50 ms prior to IR irradiation. The typical irradiation time used in the experiments is 1 s. The irradiation time is controlled using an electromechanical shutter synchronized precisely with the mass spectrometer.

3. Computational methods

Geometry optimization of various tautomers of cysteine radical cation is performed using the Gaussian 03 suite of programs. The minimum energy structures were optimized at the UB3LYP level of theory with the 6-311++G(d,p) basis set. All optimized structures were subjected to harmonic vibrational frequency analysis to characterize the stationary points as local minima. Scaling factors of 0.976 and 0.955 were applied on the calculated frequencies in the 1000–2000 and 2900–3700 cm^{-1} spectral region, respectively, on the basis of the good agreement between the experimental and computed frequencies.[15] Finally, the calculated spectra were convoluted by a Lorentzian function of full width 20 and 13 cm^{-1} in the 1000–2000 and 2900–3700 cm^{-1} spectral region, respectively, for consistency with the experimental spectral resolution.

Results and discussions

1. Low energy tautomers of cysteine radical cation

A survey of the several possible tautomeric structures corresponding to cysteine radical cation was conducted by previous theoretical studies.[9,18] Besides the canonical structure, several other isomers are conceivable depending on how the formal charge (at the carbonyl oxygen, the amino nitrogen or the S atom) and the radical center (on the S atom, the α-carbon or even an O- or N-atom) are placed within the molecule.

Fig. 1 shows the four lowest energy tautomers of cysteine radical cation calculated using the UB3LYP/6-311++G(d,p) level of theory. The structure and the relative energy of these tautomers are quite similar to the ones obtained by Ryzhov *et al.* in their work on this radical cation.[9] Intramolecular hydrogen bond formation is observed in three of these tautomers, as depicted in Fig. 1 with the respective interatomic distances.

The canonical structure (**IV**) in which both the positive charge and the radical are formally localized on the sulfur atom is not the most stable one, which instead is **I**. This tautomer at the global minimum is formally obtained from

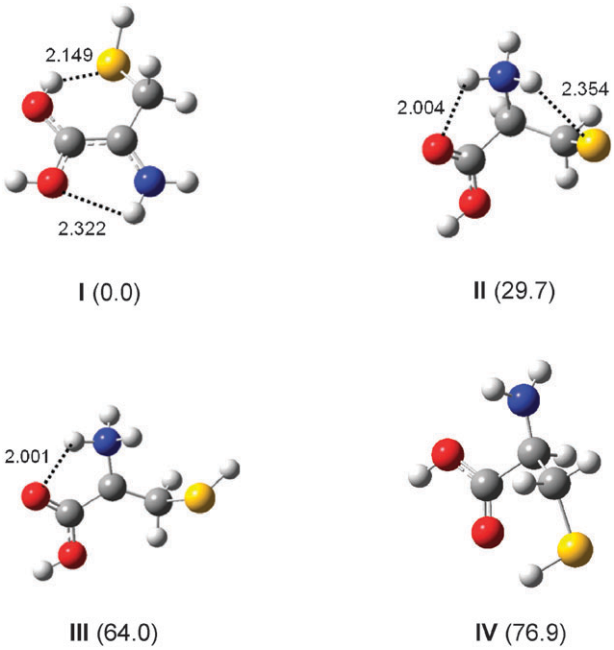

Fig. 1 Low energy isomers of cysteine radical cation. The geometry optimization was performed at UB3LYP/6-311++G(d,p) level of theory. The interatomic distances of hydrogen bonds are given in Å and the relative energies (in parentheses) are in kJ mol^{-1}.

the canonical structure by a hydrogen atom transfer from the α-carbon to the carboxyl group. In this ion the radical site is attached to both a strong π-electron donor (NH_2) and a strong π-electron withdrawing ($C(OH)_2^+$) group, thus yielding a planar 'captodative' radical, gaining stability by the delocalization of both the spin and the charge.[18a,19] A remarkable example is provided by the structure of a captodative α-radical ion, the histidine radical cation, that has been confirmed by IRMPD spectroscopy and density functional calculations.[15] The distonic ion **II**, characterized by a protonated amino group and a radical site on sulfur, is the expected product of the homolysis reaction (1). For this S-NO cleavage process a bond dissociation energy of 105.8 kJ mol^{-1} has been calculated.[9] Species **III** is an α-carbon radical with a protonated amino group.

2. Photodissociation mass spectra

$Cys^{\bullet+}$ ions formed either directly from ESI of an acidic solution of S-nitrosocysteine or from the CID of protonated S-nitrosocysteine have been sampled by IRMPD spectroscopy, showing consistently common features. The absorption of multiple photons in resonance with an active IR mode raises the energy content of the ion up to a dissociation threshold. Fig. 2a shows the mass spectrum of $Cys^{\bullet+}$ recorded upon irradiation by the IR FEL beam at 1450 cm^{-1}. In the inset of this figure, a vertically expanded mass spectrum in 50–100 Da range is shown. Fragment ions can be observed at m/z 76 (loss of $^{\bullet}COOH$, 45 Da), m/z 75 (loss of CH_2S, 46 Da), and m/z 74 (loss of $^{\bullet}CH_2SH$, 47 Da). An additional weak signal at m/z 87 has been assigned to the loss of H_2S (34 Da). These fragment ions have already been described in the CID mass spectrum of $Cys^{\bullet+}$ and assigned to the respective dissociation products

with the aid of deuterium labelling experiments,[9] while several possible fragmentation paths have been examined in theoretical studies.[18]

This same fragmentation pattern was found for all the vibrational bands observed in the 1000–2000 cm^{-1} region. In contrast, noticeable differences are observed when the molecular ion is irradiated at 3556 cm^{-1}, as shown in Fig. 2b. Whereas the fragments at m/z 76, 75, and 74 are consistent with earlier observations, the ion at m/z 87 is not present and a new strong signal at m/z 57 is observed. Presently, there is not a clearcut explanation for this behavior. Different IRMPD mass spectra recorded in correspondence with different absorption bands may arise from secondary photofragmentation processes affecting one primary photofragment.[20] For example, the IRMPD process undergone by protonated benzaldehyde has been found to yield $C_6H_7^+$ ions together with $C_6H_5^+$.[20a] However, the latter photofragment is observed only in a limited number of the IRMPD bands, namely at those wavelengths where protonated benzene presents active IR modes. This observation was found consistent with a consecutive IRMPD process undergone by the primary $C_6H_7^+$ fragments that could thus be assigned a protonated benzene structure.

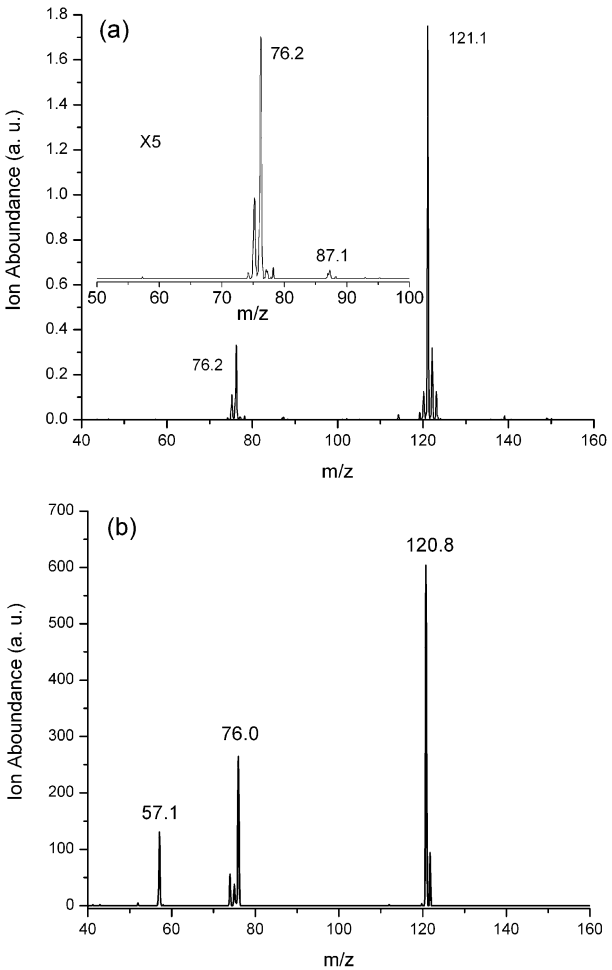

Fig. 2 Infrared induced mass spectra (Ion abundances in arbitrary units) of cysteine radical cation recorded at (a) 1450 cm^{-1} and (b) 3556 cm^{-1}.

It is also relevant to remind that in the IRMPD process the efficiency of fragmentation depends on various factors, among which one should take into account the specific features of the potential energy surface, the time dependence of the internal energy distribution and the efficiency of energy transfer from the resonantly excited vibrational mode to the rest of the molecule through the intramolecular vibrational relaxation (IVR) process.[11,21] It is conceivable that multiple photon absorption by a mode with a high oscillator strength may open the way to alternative fragmentation paths.

The ion abundances in the mass spectra recorded at each wavenumber allow calculating the IRMPD yield, $R = -\log(I_{parent}/(I_{parent} + \sum I_{fragment}))$, where I_{parent} and $I_{fragment}$ are the ion signal intensities for the parent and fragment ions, respectively. R is plotted against the wavenumber of the IR radiation to deliver the IRMPD spectra described in the following sections.

3. IRMPD spectrum

A. Mid-IR range. Fig. 3a shows the IRMPD spectrum of $Cys^{\bullet+}$ in the wavenumber range of 1000–2000 cm^{-1}. Three bands can be clearly seen in the spectrum at 1773, 1445, and 1152 cm^{-1}. A shoulder at approximately 1174 cm^{-1} is also observed in the higher energy side of the band at 1152 cm^{-1}. In order to interpret the vibrational modes corresponding to these IRMPD bands, Fig. 3b–e shows the IR spectra calculated for the four minimum energy structures. The vibrational frequencies are scaled with a factor of 0.976, known to be appropriate for DFT comparisons with IRMPD features in this spectral region.[15] Table 1 lists the IRMPD and computed spectral features for all the cysteine radical cation tautomers considered in this work.

The comparison of the IRMPD spectrum with the calculated IR spectra is straightforward. The IR spectrum shown in Fig. 3c, corresponding to the second minimum structure, neatly accounts for the IRMPD spectrum. Among the most active modes for tautomer **II**, the characteristic C=O stretch appears at 1773 cm^{-1} which is in perfect agreement with the experimentally observed band at 1773 cm^{-1}. For the most stable structure, this characteristic band is absent whereas for tautomers **III** and **IV**, this band appears at 1667 and 1711 cm^{-1}, respectively, which means a red shift of 106 and 62 cm^{-1} with respect to the experimentally observed band. The second strong feature in the IRMPD spectrum is at 1445 cm^{-1}. The IR spectrum of tautomer **II** shows a band at 1448 cm^{-1}. This band corresponds to the umbrella mode of NH_3 group. For tautomers **I** and **IV**, this band is missing. For tautomer **III**, three closely spaced bands are observed at 1427, 1414 and 1408 cm^{-1}. The band at 1427 cm^{-1} corresponds to the NH_3 umbrella mode whereas the other two bands at 1414 and 1408 cm^{-1} are the coupled vibrations of the NH_3 umbrella mode with the CH_2 bending and COH bending modes. All these transitions are red shifted compared to the band observed in the IRMPD spectrum. In tautomer **II**, two closely spaced bands are observed at 1174 and 1152 cm^{-1} in the calculated IR spectrum. These two bands are in nice agreement with the bands observed at 1174 and 1152 cm^{-1} in

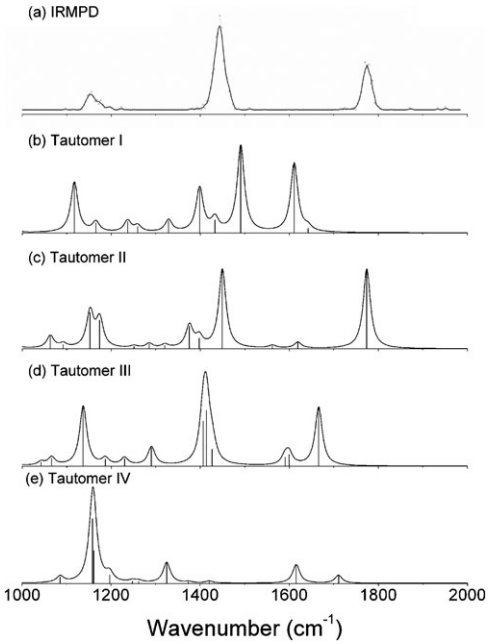

Fig. 3 IRMPD spectrum and the theoretically calculated spectra for cysteine radical cation in the molecular fingerprint region.

the IRMPD spectrum. These bands correspond to coupled bending motions in the molecular ion. Overall, the modes appear as flexing of the molecular ion skeleton. A similar vibration in tautomer **IV** is calculated to appear at 1159 cm^{-1}. In tautomer **I** and **III**, we could not find this same skeletal flexing.

Upon comparing the experimental IRMPD with the calculated IR spectra, we conclude that although tautomer **I** presents the most stable structure of cysteine radical cation, tautomer **II**, at a relative energy of 29.7 kJ mol^{-1} compared to tautomer **I**, is the species actually sampled in the gas phase.

B. 2900–3700 cm^{-1} spectral range. Fig. 4a shows the IRMPD spectrum of cysteine radical cation recorded in the 2900–3700 cm^{-1} spectral range. The calculated IR spectra in this region are displayed in Fig. 4b–e. The frequencies of the calculated and experimental spectral features are listed in Table 1. This spectral region is characteristic of O–H, N–H and C–H stretching vibrations. As previously observed in the molecular fingerprint region, here as well, the comparison of the experimental IRMPD and the calculated IR spectrum is straightforward. In the IRMPD spectrum two distinct bands are observed at 3548 and 3343 cm^{-1}. These bands show very good agreement in their spectral position with the calculated IR features for tautomer **II**. The first band on the higher energy side for this tautomer appears at 3550 cm^{-1}. This band is due to the free O–H stretch in the radical cation. For the most stable tautomer **I**, two O–H stretches were predicted at 3567 and 3027 cm^{-1}. The second O–H band shows a red shift of 540 cm^{-1} compared to the first O–H stretch. This is due to the hydrogen bond established between the hydroxyl hydrogen and the S atom. For tautomers **III** and **IV**, there is just one free O–H band at 3564 and 3535 cm^{-1}, respectively. While the IRMPD feature at 3343 cm^{-1} matches very well with the N–H stretching mode of tautomer **II** expected at 3336 cm^{-1}, the highly active modes predicted at 3151 and 2998 cm^{-1} are apparently missing. However, these two modes are associated to N–H stretching vibrations involved in hydrogen bonding with the carbonyl oxygen or the S atom, respectively. This binding motif is known to cause a red shift accompanied by a remarkable broadening of the associated IRMPD band.[22] The extent may be so pronounced that the band may not emerge from background noise any longer. In the IRMPD spectrum of $Cys^{\bullet+}$ presently reported in Fig. 4a, a broad signal of low intensity may be recognized at 3145–3155 cm^{-1}. For tautomer **I**, two symmetric and one antisymmetric N–H stretches appear at 3392 and 3504 cm^{-1}, respectively, which do not find a counterpart in the experimental spectrum. Similarly, any matching with the IRMPD resonances is missing when the N–H transitions for tautomer **III** (appearing at 3248, 3158 and 3081 cm^{-1}) and for tautomer **IV** (two N–H antisymmetric and a symmetric band appearing at 3520 and 3406 cm^{-1}, respectively) are considered.

Overall, data collected in Fig. 4 and Table 1 point to tautomer **II** as the only species appreciably present in the sampled ion population.

Table 1 Spectral position of IRMPD bands and calculated IR resonances (in cm^{-1}) observed in the molecular fingerprint region as well as in the O–H/N–H stretching region

IRMPD	Tautomer I	Tautomer II	Tautomer III	Tautomer IV	Mode description
3548	3567	3550	3564	3535	OH free
	3504			3520	NH2 antisym
	3392			3406	NH2 sym
	3027 (OH–S)				OH
3343		3336	3248		NH
3145–3155		3151 (NH–O)	3158 (NH–O)		NH
		2998 (NH–S)	3081		NH
1773		1773	1667	1711	C=O
	1610			1614	NH2 scissoring
	1492				
1445		1448	1427		NH3 umbrella
			1414		NH3 umbrella + CH2 bend
			1408		NH3 umbrella + CH2 bend + COH bend
1174		1174		1324	COH bending
1152		1152		1159	Skeletal flexing
			1136		COH bend + CH wagging

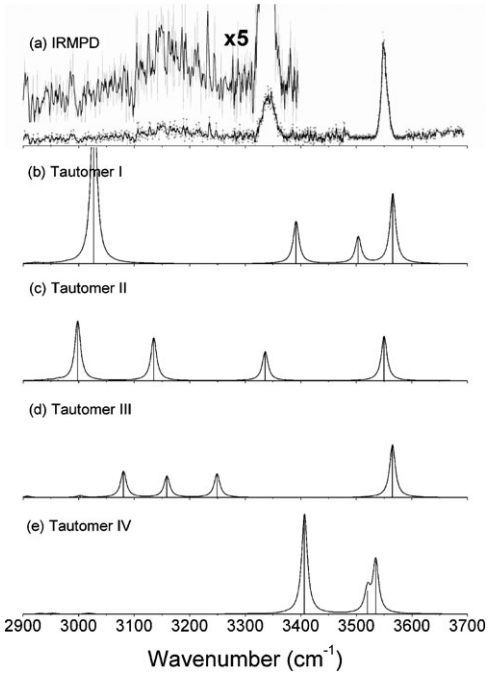

Fig. 4 IRMPD spectrum and theoretically calculated spectra for cysteine radical cation in the N–H/O–H stretching region.

Conclusions

A cysteine radical cation has been unambiguously characterized by IRMPD spectroscopy in two different spectral regions, namely the 1000–2000 cm^{-1} region, accessed by the CLIO FEL light source, and the 2900–3700 cm^{-1} spectral range, inspected by using an OPO/OPA laser source. In the latter experiments we made use of a newly assembled apparatus coupling tunable IR laser light of fairly high fluence with an ion trap mass spectrometer. The requisite of fluence is justified by the multiple photon character of the process being exploited. Indeed, the photofragmentation process that is observed throughout the wavenumber range covered in the reported IRMPD experiments is activated by the absorption of multiple photons, as required to reach a threshold energy for dissociation in excess of 100 kJ mol^{-1}, even for the most readily accessed channel of $^{\bullet}$COOH loss.[9,18] This situation holds also in the high energy side of the explored IR spectrum where the energy of a photon at 3600 cm^{-1} is 43 kJ mol^{-1}.

In contrast with the important role of oxidized forms of cysteine residues in biological processes, obtaining $Cys^{\bullet+}$ ions in the gas phase is not a trivial matter. The homolytic S–NO bond rupture in protonated S-nitrosocysteine has provided an entry to this otherwise elusive species.[9] CID mass spectrometry, supported by labelling experiments and detailed DFT calculations of ionic structures and dissociation reaction profiles, has provided valuable means to obtain a structural characterization. The specific tautomeric structure of sampled $Cys^{\bullet+}$ ions is now elucidated by combining the IRMPD investigation in two diagnostic portions of the IR spectrum with the results of DFT calculations. There is a very good correspondence of predicted and calculated frequencies and the relative intensities are approximately matched when the IRMPD features are compared with the IR spectrum calculated for tautomer **II**, the distonic ion with the charge on a protonated amino group and the radical site at the sulfur atom. This species is not the most stable one, placed in a relative minimum at 29.7 kJ mol^{-1} above the energy of the most stable isomer, the captodative radical ion **I**. The canonical structure **IV** is still higher in energy at 76.9 kJ mol^{-1}. It may be argued that the tautomer **II** structure of the observed $Cys^{\bullet+}$ ions may be an obvious consequence of the route by which the ions were formed, namely the homolytic dissociation of the S–NO bond of protonated S-nitroso cysteine. This reaction (eqn (1)) leads directly to $H_3N^+CH(CH_2S^{\bullet})CO_2H$ ions along a path calculated to be 105.8 kJ mol^{-1} endothermic.[9] The associated activation barrier is 128.4 kJ mol^{-1} and any excess energy released in the so-formed product ion should not allow it to rearrange into the most stable tautomer **I**. Relatively high barriers for the mutual rearrangement of tautomers **I–IV** combined with a low free energy for dissociation *via* the loss of $^{\bullet}$COOH[9,18*a*] have permitted the successful characterization of the observed $Cys^{\bullet+}$ ions by IRMPD spectroscopy (for example tautomerism between **II** and **I** requires an intermediate step which has a barrier 222.6 kJ mol^{-1} to be compared with the 118.0 kJ mol^{-1} required for the loss of of $^{\bullet}$COOH, energy values relative to **II**).[18*a*] It may thus be safely anticipated that when alternative routes to tautomers **I–IV** are envisioned, IRMPD spectroscopy will provide the means to discriminate between the possible isomeric structures. At the same time the premises are laid that IRMPD spectroscopy may prove a powerful tool for investigating more complex cysteine-containing biomolecules such as the radical cations of cysteine-containing peptides whose gas-phase unimolecular chemistry and fragmentation behavior are described in a thorough, recent study.[23]

Acknowledgements

This work was supported by the CNRS (PICS program), by the Italian Ministero dell'Istruzione, dell'Università e della Ricerca and by the European Commission (EPITOPES, Project No. 15637) who also provided travel funding to M.E.C. and B.C. for access to the European multi-user facility CLIO. We thank Prof. Jean-Michel Ortega for the support of the CLIO team and are grateful to Prof. Debora Scuderi, Prof. Antonello Filippi, Dr Flaminia Rondino and Dr Annito Di Marzio for the competence and efforts spent in setting up the OPO/OPA laser source—mass spectrometer apparatus at the Università di Roma "La Sapienza".

References

1 (*a*) J. Stubbe and W. A. van der Donk, *Chem. Rev.*, 1998, **98**, 705–762; (*b*) B. S. Berlett and E. R. Stadtman, *J. Biol. Chem.*, 1997, **272**, 20313–20316; (*c*) F. Himo and P. E. M. Siegbahn, *Chem. Rev.*, 2003, **103**, 2421–2456; (*d*) M. H. V. Huynh and T. J. Meyer, *Chem. Rev.*, 2007, **107**, 5004–5064; (*e*) K. Westerlund, B. W. Berry, H. K. Privett and C. Tommos, *Biochim. Biophys. Acta, Bioenerg.*, 2005, **1707**, 103–116; (*f*) C. Schoeneich, *Chem. Res. Toxicol.*, 2008, **21**, 1175–1179.
2 A. C. Hopkinson, *Mass Spectrom. Rev.*, 2009, **28**, 655–671.
3 (*a*) G. Junk and H. Svec, *J. Am. Chem. Soc.*, 1963, **85**, 839–845; (*b*) K. Biemann and J. A. McCloskey, *J. Am. Chem. Soc.*, 1962, **84**, 3192–3193.

4 (*a*) W. Cui, Y. Hu and C. Lifshitz, *Eur. Phys. J. D*, 2002, **20**, 565–571; (*b*) C. H. Becker and K. J. Wu, *J. Am. Soc. Mass Spectrom.*, 1995, **6**, 883–888; (*c*) J. Grotemeyer and E. W. Schlag, *Org. Mass Spectrom.*, 1988, **23**, 388–396.

5 (*a*) R. A. Zubarev, N. L. Kelleher and F. W. McLafferty, *J. Am. Chem. Soc.*, 1998, **120**, 3265–3266; (*b*) R. A. Zubarev, *Mass Spectrom. Rev.*, 2003, **22**, 57–77; (*c*) F. Turecek, *J. Am. Chem. Soc.*, 2003, **125**, 5954–5963; (*d*) A. T. Iavarone, K. Paech and E. R. Williams, *Anal. Chem.*, 2004, **76**, 2231–2238; (*e*) E. A. Syrstad and F. Turecek, *J. Am. Soc. Mass Spectrom.*, 2005, **16**, 208–224.

6 V. Blagojevic, S. Petrie and D. K. Bohme, *Mon. Not. R. Astron. Soc.*, 2003, **339**, L7–L11.

7 (*a*) I. K. Chu, C. F. Rodriquez, T.-C. Lau, A. C. Hopkinson and K. W. M. Siu, *J. Phys. Chem. B*, 2000, **104**, 3393–3397; (*b*) I. K. Chu, C. F. Rodriquez, A. C. Hopkinson, K. W. M. Siu and T.-C. Lau, *J. Am. Soc. Mass Spectrom.*, 2001, **12**, 1114–1119; (*c*) C. K. Barlow, S. Wee, W. D. McFadyen and R. A. J. O'Hair, *Dalton Trans.*, 2004, 3199–3204; (*d*) C. K. Barlow, W. D. McFadyen and R. A. J. O'Hair, *J. Am. Chem. Soc.*, 2005, **127**, 6109–6115; (*e*) C. K. Barlow, D. Moran, L. Radom, W. D. McFadyen and R. A. J. O'Hair, *J. Phys. Chem. A*, 2006, **110**, 8304–8315; (*f*) Y. Ke, J. Zhao, U. H. Verkerk, A. C. Hopkinson and K. W. M. Siu, *J. Phys. Chem. B*, 2007, **111**, 14318–14328; (*g*) F. Tureček, *Mass Spectrom. Rev.*, 2007, **26**, 563–582; (*h*) C.-K. Siu, Y. Ke, Y. Guo, A. C. Hopkinson and K. W. M. Siu, *Phys. Chem. Chem. Phys.*, 2008, **10**, 5908–5918; (*i*) J. Laskin, Z. Yang and I. K. Chu, *J. Am. Chem. Soc.*, 2008, **130**, 3218–3230.

8 (*a*) G. Hao and S. S. Gross, *J. Am. Soc. Mass Spectrom.*, 2006, **17**, 1725–1730; (*b*) F. S. Taldone, M. Tummala, E. J. Goldstein, V. Ryzhov, K. Ravi and S. M. Black, *Nitric Oxide*, 2005, **13**, 176–187; (*c*) Y. Wang, T. Liu, C. Wu and H. Li, *J. Am. Soc. Mass Spectrom.*, 2008, **19**, 1353–1360.

9 V. Ryzhov, A. K. Y. Lam and R. A. J. O'Hair, *J. Am. Soc. Mass Spectrom.*, 2009, **20**, 985–995.

10 J. Zhao, C. M. D. Ng, I. K. Chu, K. W. M. Siu and A. C. Hopkinson, *Phys. Chem. Chem. Phys.*, 2009, **11**, 7629–7639.

11 (*a*) T. D. Fridgen, *Mass Spectrom. Rev.*, 2009, **28**, 586–607; (*b*) J. R. Eyler, *Mass Spectrom. Rev.*, 2009, **28**, 448–467; (*c*) M. A. Duncan, *Int. J. Mass Spectrom.*, 2008, **272**, 99–118; (*d*) N. C. Polfer and J. Oomens, *Mass Spectrom. Rev.*, 2009, **28**, 468–494; (*e*) N. C. Polfer and J. Oomens, *Phys. Chem. Chem. Phys.*, 2007, **9**, 3804–3817; (*f*) N. R. Walker, R. S. Walters and M. A. Duncan, *New J. Chem.*, 2005, **29**, 1495–1503; (*g*) O. Dopfer, *Z. Phys. Chem.*, 2005, **219**, 125–168; (*h*) M. A. Duncan, *Int. Rev. Phys. Chem.*, 2003, **22**, 407–435; (*i*) L. MacAleese and P. Maitre, *Mass Spectrom. Rev.*, 2007, **26**, 583–605; (*j*) J. Oomens, B. G. Sartakov, G. Meijer and G. von Helden, *Int. J. Mass Spectrom.*, 2006, **254**, 1–19.

12 W. Jones, P. Boissel, B. Chiavarino, M. E. Crestoni, S. Fornarini, J. Lemaire and P. Maitre, *Angew. Chem., Int. Ed.*, 2003, **42**, 2057–2059.

13 (*a*) B. Chiavarino, M. E. Crestoni, S. Fornarini, J. Lemaire, L. MacAleese and P. Maitre, *ChemPhysChem*, 2005, **6**, 437–440; (*b*) O. Dopfer, N. Solca, J. Lemaire, P. Maitre, M. E. Crestoni and S. Fornarini, *J. Phys. Chem. A*, 2005, **109**, 7881–7887; (*c*) O. Dopfer, J. Lemaire, P. Maitre, B. Chiavarino, M. E. Crestoni and S. Fornarini, *Int. J. Mass Spectrom.*, 2006, **249–250**, 149–154; (*d*) B. Chiavarino, M. E. Crestoni, S. Fornarini, J. Lemaire, P. Maitre and L. MacAleese, *J. Am. Chem. Soc.*, 2006, **128**, 12553–12561; (*e*) U. J. Lorenz, J. Lemaire, P. Maitre, M. E. Crestoni, S. Fornarini and O. Dopfer, *Int. J. Mass Spectrom.*, 2007, **267**, 43–53; (*f*) B. Chiavarino, M. E. Crestoni, S. Fornarini, F. Lanucara, J. Lemaire and P. Maitre, *Angew. Chem., Int. Ed.*, 2007, **46**, 1995–1998; (*g*) B. Chiavarino, M. E. Crestoni, S. Fornarini, F. Lanucara, J. Lemaire, P. Maitre and D. Scuderi, *Int. J. Mass Spectrom.*, 2008, **270**, 111–117; (*h*) B. Chiavarino, M. E. Crestoni, S. Fornarini, F. Lanucara, J. Lemaire, P. Maitre and D. Scuderi, *ChemPhysChem*, 2008, **9**, 826–828; (*i*) B. Chiavarino, M. E. Crestoni, S. Fornarini, F. Lanucara, J. Lemaire, P. Maitre and D. Scuderi, *Chem.–Eur. J.*, 2009, **15**, 8185–8195, S8185/1–S8185/3.

14 (*a*) R. Wu and T. B. McMahon, *ChemPhysChem*, 2008, **9**, 2826–2835; (*b*) R. Wu and T. B. McMahon, *J. Am. Chem. Soc.*, 2008, **130**, 3065–3078; (*c*) R. Wu and T. B. McMahon, *Angew. Chem., Int. Ed.*, 2007, **46**, 3668–3671; (*d*) B. Lucas, G. Gregoire, J. Lemaire, P. Maitre, F. Glotin, J. P. Schermann and C. Desfrancois, *Int. J. Mass Spectrom.*, 2005, **243**, 105–113; (*e*) A. Simon, L. MacAleese, P. Maitre, J. Lemaire and T. B. McMahon, *J. Am. Chem. Soc.*, 2007, **129**, 2829–2840; (*f*) C. Kapota, J. Lemaire, P. Maitre and G. Ohanessian, *J. Am. Chem. Soc.*, 2004, **126**, 1836–1842; (*g*) R. C. Dunbar, A. C. Hopkinson, J. Oomens, C.-K. Siu, K. W. M. Siu, J. D. Steill, U. H. Verkerk and J. Zhao, *J. Phys. Chem. B*, 2009, **113**, 10403–10408; (*h*) J. Oomens, J. D. Steill and B. Redlich, *J. Am. Chem. Soc.*, 2009, **131**, 4310–4319; (*i*) J. T. O'Brien, J. S. Prell, J. D. Steill, J. Oomens and E. R. Williams, *J. Phys. Chem. A*, 2008, **112**, 10823–10830; (*j*) M. F. Bush, J. Oomens, R. J. Saykally and E. R. Williams, *J. Am. Chem. Soc.*, 2008, **130**, 6463–6471; (*k*) P. B. Armentrout, M. T. Rodgers, J. Oomens and J. D. Steill, *J. Phys. Chem. A*, 2008, **112**, 2248–2257; (*l*) M. T. Rodgers, P. B. Armentrout, J. Oomens and J. D. Steill, *J. Phys. Chem. A*, 2008, **112**, 2258–2267; (*m*) M. W. Forbes, M. F. Bush, N. C. Polfer, J. Oomens, R. C. Dunbar, E. R. Williams and R. A. Jockusch, *J. Phys. Chem. A*, 2007, **111**, 11759–11770; (*n*) N. C. Polfer, J. Oomens and R. C. Dunbar, *Phys. Chem. Chem. Phys.*, 2006, **8**, 2744–2751.

15 J. Steill, J. Zhao, C.-K. Siu, Y. Ke, U. H. Verkerk, J. Oomens, R. C. Dunbar, A. C. Hopkinson and K. W. M. Siu, *Angew. Chem., Int. Ed.*, 2008, **47**, 9666–9668.

16 L. Grossi and Pier Carlo Montevecchi, *J. Org. Chem.*, 2002, **67**, 8625–8630 and references cited therein.

17 P. Maitre, J. Lemaire and D. Scuderi, *Phys. Scr.*, 2008, **78**, 058111, 058111/1–058111/6.

18 (*a*) J. Zhao, K. W. M. Siu and A. C. Hopkinson, *Phys. Chem. Chem. Phys.*, 2008, **10**, 281–288; (*b*) S. Simon, A. Gil, M. Sodupe and J. Bertran, *THEOCHEM*, 2005, **727**, 191–197; (*c*) A. Gil, S. Simon, L. Rodriguez-Santiago, J. Bertran and M. Sodupe, *J. Chem. Theory Comput.*, 2007, **3**, 2210–2220.

19 (*a*) R. Sustmann and H. G. Korth, *Adv. Phys. Org. Chem.*, 1991, **26**, 131–78; (*b*) A. K. Croft, C. J. Easton and L. Radom, *J. Am. Chem. Soc.*, 2003, **125**, 4119–4124.

20 (*a*) B. Chiavarino, M. E. Crestoni, S. Fornarini, O. Dopfer, J. Lemaire and P. Maitre, *J. Phys. Chem. A*, 2006, **110**, 9352–9360; (*b*) J. M. Bakker, T. Besson, J. Lemaire, D. Scuderi and P. Maitre, *J. Phys. Chem. A*, 2007, **111**, 13415–13424; (*c*) J. Lemaire, P. Boissel, M. Heninger, G. Mauclaire, G. Bellec, H. Mestdagh, A. Simon, S. Le Caer, J. M. Ortega, F. Glotin and P. Maitre, *Phys. Rev. Lett.*, 2002, **89**, 273002–273004; (*d*) A. Simon, W. Jones, J.-M. Ortega, P. Boissel, J. Lemaire and P. Maitre, *J. Am. Chem. Soc.*, 2004, **126**, 11666–11674.

21 (*a*) R. C. Dunbar, D. T. Moore and J. Oomens, *J. Phys. Chem. A*, 2006, **110**, 8316–8326; (*b*) J. Oomens, D. T. Moore, G. Meijer and G. von Helden, *Phys. Chem. Chem. Phys.*, 2004, **6**, 710–718.

22 (*a*) J. M. Bakker, J.-Y. Salpin and P. Maitre, *Int. J. Mass Spectrom.*, 2009, **283**, 214–221; (*b*) J. M. Bakker, R. K. Sinha, T. Besson, M. Brugnara, P. Tosi, J.-Y. Salpin and P. Maitre, *J. Phys. Chem. A*, 2008, **112**, 12393–12400; (*c*) A. Kamariotis, O. V. Boyarkin, S. R. Mercier, R. D. Beck, M. F. Bush, E. R. Williams and T. R. Rizzo, *J. Am. Chem. Soc.*, 2006, **128**, 905–916; (*d*) Y.-S. Wang, H.-C. Chang, J.-C. Jiang, S. H. Lin, Y. T. Lee and H.-C. Chang, *J. Am. Chem. Soc.*, 1998, **120**, 8777–8788.

23 A. K. Y. Lam, V. Ryzhov and R. A. J. O'Hair, *J. Am. Soc. Mass Spectrom.*, 2010, **21**, DOI: 10.1016/j.jasms.2010.01.027, in press.

